

DMD #17905

Generation and functional characterization of mice with a disrupted *glutathione S-transferase, theta 1* gene

Kazunori Fujimoto, Shingo Arakawa, Toshiyuki Watanabe, Hiroaki Yasumo, Yosuke Ando, Wataru Takasaki, Sunao Manabe, Takashi Yamoto, Sen-ichi Oda

Medicinal Safety Research Laboratories, Daiichi Sankyo Co., Ltd., 717 Horikoshi, Fukuroi, Shizuoka 437-0065, Japan (KF, SA, TW, YA, WT, SM, TY)

Exploratory Research Laboratories I, Daiichi Sankyo Co., Ltd., 1-2-58 Hiromachi, Shinagawa, Tokyo 140-8710, Japan (HY)

Graduate School of Bioagricultural Sciences, Nagoya University, Furo-cho, Chikusa, Nagoya 464-8601, Japan (KF, SO)

DMD #17905

Running title:

Functional characterization of *Gstt1*-null mice

Corresponding author:

Kazunori Fujimoto, Medicinal Safety Research Laboratories, Daiichi Sankyo Co., Ltd., 717

Horikoshi, Fukuroi, Shizuoka 437-0065, Japan, Phone: +81-538-42-4356, Fax: +81-538-42-4350,

E-mail: fujimoto.kazunori.wr@daiichisankyo.co.jp

Number of text pages: 28

Number of figures: 5

Number of tables: 1

Number of references: 32

Words in Abstract: words: 231

Words in Introduction: words: 458

Words in Discussion: words: 1061

Abbreviations:

GSTT1, glutathione S-transferase theta 1; 2D-DIGE/MS, 2-dimensional fluorescence difference gel electrophoresis/mass spectrometry analysis; EPNP, 1,2-epoxy-3-(p-nitrophenoxy)propane; DCM, dichloromethane; BCNU, 1,3-bis(2-chloroethyl)-1-nitrosourea; CDNB, 1-choloro-2,4-dinitrobenzene.

DMD #17905

Abstract

Glutathione S-transferase Theta 1 (GSTT1) has been regarded as one of the key enzymes involved in phase II reactions because of its unique substrate specificity. In this study, we generated mice with disrupted *glutathione S-transferase, Theta 1 (Gstt1)* gene (*Gstt1*-null mice) by gene targeting, and analyzed the metabolic properties in cytosolic and *in vivo* studies. The resulting *Gstt1*-null mice failed to express the *Gstt1* mRNA and GSTT1 protein by RT-PCR analysis and 2-dimensional fluorescence difference gel electrophoresis/mass spectrometry analysis, respectively. However, the *Gstt1*-null mice appeared to be normal and were fertile. In an enzymatic study using cytosolic samples from the liver and kidney, GST activity toward 1,2-epoxy-3-(p-nitrophenoxy)propane (EPNP), dichloromethane (DCM) and 1,3-bis(2-chloroethyl)-1-nitrosourea (BCNU) was markedly lower in *Gstt1*-null mice than in the wild-type controls, in spite of there being no difference in GST activity toward 1-chloro-2,4-dinitrobenzene between *Gstt1*-null mice and the wild-type controls. *Gstt1*-null mice had GST activity of only 8.7 to 42.1% of the wild-type controls to EPNP, less than 2.2% of the wild-type controls to DCM and 13.2 to 23.9% of the wild-type controls to BCNU. Plasma BCNU concentrations after a single intraperitoneal administration of BCNU to *Gstt1*-null mice were significantly higher and there was a larger AUC_{5-60 min} (male, 2.30 times; female, 2.28 times, versus the wild-type controls) based on the results. In conclusion, *Gstt1*-null mice would be useful as an animal model of humans with *GSTT1*-null genotype.

DMD #17905

Introduction

Glutathione *S*-transferases (GSTs) form a superfamily that is characterized by catalysis of the conjugation of glutathione (GSH) with various electrophilic compounds. At least seven distinct classes (Alpha, Mu, Pi, Theta, Zeta, Omega and Sigma) of soluble GSTs have been identified so far, according to substrate specificity, chemical affinity, structure and the kinetic behavior of the enzyme (Mannervik *et al.*, 1985; Meyer *et al.*, 1991; Board *et al.*, 1997; Board *et al.*, 2000; Jowsey *et al.*, 2001). Theta class GSTs are distinguished from other classes by their failure to bind to immobilized GSH affinity matrices and their negligible activity toward 1-chloro-2,4-dinitrobenzene (CDNB), which is the substrate of various GSTs (Meyer *et al.*, 1984; Meyer *et al.*, 1991). There is a genetic polymorphism of the null genotype in the human *GSTT1* gene, with about 15% of Caucasians and 60% of Asians lacking *GSTT1* activity (Nelson *et al.*, 1995; Chen *et al.*, 1996). The relationship between the *GSTT1*-null genotype and the incidence of cancer has been investigated extensively in order to detect *GSTT1*-associated differential susceptibility toward carcinogens. Many epidemiologic investigations have shown that the *GSTT1*-null genotype is related to a slightly increased risk of cancer of the bladder and gastro-intestinal tract, and smoking-related cancer of the lung or oral cavity (Landi, 2000). However, there is no direct evidence yet that the *GSTT1*-null genotype causes carcinogenesis.

The alkylating drug 1,3-bis(2-chloroethyl)-1-nitrosourea (BCNU) is used to treat brain tumors, multiple myeloma, Hodgkin's disease and non-Hodgkin's lymphomas (Wasserman *et al.*, 1975). BCNU is thought to exert the anti-tumor effect by the formation of a chloroethyl-adduct at the *O*⁶ position of guanine bases in the DNA (Bodell *et al.*, 1984). The critical problem in BCNU treatment is the acquisition of BCNU-resistance, which is implicated in many mechanisms in the

DMD #17905

tumor cells. The major resistant factors are O^6 -alkylguanine-DNA-alkyltransferase, which repairs DNA damage by removing the alkyl groups from the O^6 position of guanine, and GSTs as a BCNU detoxifying enzyme (Bodell *et al.*, 1986; Smith *et al.*, 1989). It has been reported that human GSTM2, GSTM3 and GSTT1 have BCNU denitrosation activity (Lien *et al.*, 2002). In particular, GSTT1 displayed a much higher activity toward BCNU. The existence of a *GSTT1*-null genotype may influence both the sensitivity of tumors to BCNU and the severity of adverse side-effects of BCNU in patients. So, it is important to study the metabolic properties to BCNU in *GSTT1*-null individuals. However, there is no report about it yet.

In this study, we generated mice with a disrupted *Gstt1* gene (*Gstt1*-null mice) and analyzed the metabolic activity toward the specific substrates 1,2-epoxy-3-(p-nitrophenoxy)propane (EPNP), DCM and BCNU. Furthermore, we measured the plasma BCNU concentrations after a single intraperitoneal administration of BCNU, in order to evaluate the metabolic properties of GSTT1 to the specific substrates.

DMD #17905

Materials and Methods

Generation of *Gstt1*-null Mice

To construct the targeting vector, DNA from a W9.5 ES cell was used to amplify the *Gstt1* genomic fragments for both the 5' and 3' arms. For the 5' arm, a 4.9-kb 5'-flanking sequence of the *Gstt1* gene was cloned into the *HpaI* and *XhoI* sites of the pKO Scrambler V901 plasmid. For the 3' arm, a 2.5-kb 3'-flanking sequence of the *Gstt1* gene was cloned into the *SacII* and *Sall* sites. The primers for the 5' arm were 5'-AGACCCGGGGCCAGGACTCTGACCTGCCATATTG-3' and 5'-CCCCTCGAGCCTAATGAGCTGTGTCTAACCTCTC-3'. The primers for the 3' arm were 5'-AGACCGCGGAGGAGTGAGCCTAGTGAATCTGCTC-3' and 5'-CGCGTCGACGCCAGGTACTCGTCTACACGAGCAC-3'. For the positive negative selection, a Neomycin resistant (Neo^r) cassette from the pKO SelectNeo V800 plasmid and the *Diphtheria Toxin A chain* gene (DT) from pKO SelectDT V840 plasmid was used. All the plasmids were supplied by TAKARA BIO Inc. W9.5 ES cells (10^7) were electroporated (250 V, 500 F) with 20 μg of linearized targeting vector and selected with 250 μg (active form)/mL G418 for 8 - 10 days (Fujimoto *et al.*, 2006). G418 resistant clones were primarily screened on the 3' arm by PCR with the primer pair, NeoF3: 5'-CTGCTAAAGCGCATGCTCCAGACTGCCTTG-3' and T1R1: 5'-ACATTTCCGGTCTTACCTTATGCCACAGGG-3'. The PCR positive clones were twice checked on the 5' arm by PCR with the primer pair, GT43: 5'-ATAAGGCAGGAAAGAAGTGTTACTG-3' and NP3: 5'-AATGAGGAAATTGCATCGCATT-3'. Finally, the homologous recombination was confirmed by the direct sequence of the amplified PCR fragments on both regions using an ABI PRISM 3700 DNA Analyzer (Applied Biosystems).

DMD #17905

Chimera mice were generated using the targeted ES cell clone with a near-diploid karyotype by an aggregation method (Wood *et al.*, 1993). The ES cell clone was aggregated with two zona-pellucida free 8-cell embryos from C57BL/6J mice, and cultured for 24 h. Aggregated blastocysts were transferred into the uteros of the surrogate mothers. Male chimera mice were crossed to C57BL/6J mice, and F1 heterozygous offspring to which the targeted ES cells had contributed were identified by coat color and PCR genotyping using a NeoF3/T1R1 primer pair. Furthermore, the F1 heterozygous mice were intercrossed to produce F2 mice, which were determined to be wild-type, heterozygote or homozygote (*Gstt1*-null mice) by PCR genotyping using two forward primers (NeoRF for the mutant allele: 5'-TGCTAAAGCGCATGCTCCAGACT-3', and GSTT1-WF for the wild allele: 5'-GCATCTTGGGCACATGAACTCATG-3') and one common reverse primer (GSTT1-WR: 5'-TGAGCAGATTCAGTACTAGGCTCACTC-3'). To analyze the *Gstt1* mRNA expression, the total RNA was isolated from the livers of the *Gstt1*-null mice, the heterozygotes and the wild-type controls using a QIAGEN RNeasy Kit. After DNase I treatment, cDNA were synthesized using an oligo-dT primer and SuperScript II reverse transcriptase (Invitrogen). RT-PCR was performed using the primers specific for the mouse *Gstt1* gene (forward: 5'-GTTCTGGAGCTGTACCTGGATC-3', and reverse: 5'-AGGAACCTTATACTTGTGTGCC-3') and *beta-actin* gene (forward: 5'-ATGGAATCCTGTGGCATCCATG-3', and reverse: 5'-TAGAAGCACTTGCGGTGCACGAT-3'). The amplified RT-PCR fragments were confirmed by direct sequence using an ABI PRISM 3700 DNA Analyzer.

DMD #17905

The mice were housed under a controlled temperature ($23 \pm 1^\circ\text{C}$) with free access to water and mouse chow. The experimental protocol was approved by the Ethics Review Committee for Animal Experimentation of Sankyo Co., Ltd.

Hepatic Protein Expression Analysis by 2-dimensional fluorescence difference gel electrophoresis/mass spectrometry (2D-DIGE/MS)

Liver samples of male mice were homogenized with DIGE-compatible lysis buffer containing 30 mM Tris-HCl, 7 M urea, 2 M thiourea, 5 mM magnesium acetate, 4% (w/v) CHAPS, and 0.5 mM Pefabloc SC PLUS (Roche Diagnostics GmbH). After ultrasonic treatment, the samples were centrifuged at 850 g for 20 min at 4°C , and the supernatant was collected and centrifuged at 20,000 g for 10 min at 4°C . The protein content in the supernatants was measured by the method of Bradford. Each 50 μg of the protein extracts from *Gstt1*-null mice, the heterozygotes and the wild-type controls was labeled minimally with 400 pmol of Cy3 or Cy5, according to the manufacturer's instructions (GE Healthcare UK Ltd.). A mixture of protein extracts (50 μg) from all the liver samples used was labeled with 400 pmol of Cy2 to provide an internal standard for the normalization of spot abundance. The Cy2, Cy3 and Cy5-labeled proteins were mixed evenly. The labeled protein samples were mixed with equal volumes of 2 \times sample buffer containing 7 M urea, 2 M thiourea, 4% (w/v) CHAPS, 2% (v/v) Pharmalyte (pH 3-10) and 2.4% (v/v) DeStreak Reagent (GE Healthcare UK Ltd.), and were added to rehydration buffer containing 7 M urea, 2 M thiourea, 4% (w/v) CHAPS, 1% (v/v) Pharmalyte (pH 3-10) and 1.2% (v/v) DeStreak Reagent to make 450 μL of total sample volume. The labeled protein mixtures were applied to IPG strips (pH 3-10) (GE Healthcare UK Ltd.), and subjected to isoelectric focusing (IEF) and SDS-PAGE (12.5% polyacrylamide gels, 25 cm X 20 cm X 0.1 cm) using IPGphor IEF System and an

DMD #17905

Ettan-DALT II system, respectively, according to the manufacturer's instructions (GE Healthcare UK Ltd.).

Cy dye images were collected using a Typhoon 9400 fluorescence scanner (GE Healthcare UK Ltd.) and analyzed using DeCyder software Version 5.02 (GE Healthcare UK Ltd.). The expression level of each protein spot was evaluated by the ratio of the spot volume compared to the internal standard. Protein spots that showed significant up- or down-regulation (P value of <0.01) between *Gstt1*-null mice and the heterozygotes, *Gstt1*-null mice and the wild-type controls, or the heterozygotes and the wild-type controls in the 2D-DIGE analysis were subjected to protein identification. Protein extracts (500 μ g) were separated by IEF and SDS-PAGE in the above-mentioned manner. After migration, the gels were treated with SYPRO Ruby dye (Molecular Probes Inc.) and the protein images were visualized. The significant spots were excised from the gels using an Ettan-spot picker (GE Healthcare UK Ltd.). The gel pieces were washed twice with 50% (v/v) methanol containing 50 mM ammonium bicarbonate for 20 min, dehydrated with 75% (v/v) acetonitrile, and dried completely in a vacuum centrifuge. The proteins were digested overnight at 37 °C with sequencing grade modified trypsin solution (Promega, Madison, 10 ng/ μ L in 20 mM ammonium bicarbonate). After digestion, the peptides in each gel piece were eluted sequentially with 50% (v/v) acetonitrile with 1% (v/v) trifluoroacetic acid (TFA), 50% (v/v) acetonitrile with 0.2% (v/v) TFA, and 100% acetonitrile with sonication. The samples were concentrated with a vacuum centrifuge, and dried after desalination with C18 ZipTip pipette tips (Millipore Corp.). The peptides were resuspended in 1 μ L CHCA-saturated matrix solution containing 0.5% (v/v) TFA and 50% (v/v) acetonitrile. The 0.5 μ L peptide solution was transferred onto the MALDI target and dried. Mass spectrometry of the peptides was

DMD #17905

performed using Ettan MALDI-TOF Pro (GE Healthcare UK Ltd.). For protein identification, the obtained mass information was searched against the NCBI nr database using Ettan MALDI-TOF software Version 1.11 (GE Healthcare UK Ltd.).

Measurement of GST activities toward CDNB, EPNP, DCM and BCNU in the cytosols of the liver and kidney

The liver and kidney samples of the *Gst11*-null mice, the heterozygotes and the wild-type controls were mixed with 0.154 M potassium chloride and homogenized in an ice bath. The homogenates were centrifuged at 9,000 *g* for 20 min at 4°C, and the supernatant fraction was further centrifuged at 105,000 *g* for 1 h at 4°C to isolate the cytosolic fractions. The protein concentrations in the cytosolic fractions were determined by the method of Lowry *et al.* (1951).

The GST activity toward CDNB (GST-CDNB activity) and EPNP (GST-EPNP activity) was measured according to the method of Habig *et al.* (1974). In the measurement of GST-CDNB activity, the cytosols were diluted 30-fold with 0.154 M potassium chloride, and 0.3 mL of 20 mM GSH and 0.06 mL of the diluted cytosols were mixed in 5.34 mL of 100 mM potassium phosphate buffer (pH 6.5). After the addition of CDNB at a final concentration of 1 mM, the change in absorbance at 340 nm was measured for 1 min with a spectrophotometer. In the measurement of GST-EPNP activity, 0.3 mL of 100 mM GSH and 0.2 mL of the cytosols were mixed in 5.2 mL of 100 mM potassium phosphate buffer (pH 6.5). After the addition of EPNP solution (10 mM in ethanol) at a final concentration of 0.5 mM, the change in absorbance at 360 nm was measured for 2 min with a spectrophotometer. The GST-CDNB and GST-EPNP activities were expressed as the amount of CDNB-GSH and EPNP-GSH conjugate moles formed per unit weight of protein per unit of time (nmol/min/mg protein), respectively.

DMD #17905

The GST activity toward DCM (GST-DCM activity) and BCNU (GST-BCNU activity) were measured according to the method of Nash *et al.* (1953) and Talcott and Levin (1983), respectively. Briefly, the cytosols of the liver and kidney were diluted 5-fold and 2-fold with 0.154 M potassium chloride, respectively. In the measurement of GST-DCM activity, 0.5 mL of reaction buffer (10 mM GSH, 20 mM Tris/HCl, pH 7.4) was mixed with 0.1 mL of the diluted cytosols and 2 μ L of DCM. After incubation for 30 min at 37 °C, this reaction was mixed thoroughly with 0.201 mL of a 20% trichloroacetic acid solution and centrifuged for 2 min at 16000 g. An amount of 0.1 mL of the supernatant was mixed with 0.1 mL Nash-reagent (15 g ammonium acetate, 0.2 mL acetylacetone, 0.3 mL acetic acid brought to a volume of 100 mL with distilled water) and incubated at 37 °C. After 60 min, the absorption at 412 nm was measured using a spectrophotometer. The GST-DCM activity was expressed as the amount of formaldehyde moles formed per unit weight of protein per unit of time (nmol/min/mg protein). In the measurement of GST-BCNU activity, 0.65 mL of 0.1 M phosphate buffer (pH 7.4) with 5 mM GSH was mixed with 0.1 mL of the diluted cytosols and 7.5 μ L of 200 mM BCNU. After the incubation for 20 min at 37 °C, this reaction was mixed thoroughly with 0.75 mL of chloroform. After 5 min centrifugation at 21,500 g, 0.5 mL of the aqueous phase was extracted with 0.75 mL of chloroform again. After the second extraction, 0.2 mL of the aqueous phase was mixed with 0.4 mL of 50 mM sulfanilamide and 0.5 mM N-(1-naphthyl)ethylenediamine dihydrochloride dissolved in 3M HCl and incubated at 55 °C. After 20 min, the absorption at 540 nm was measured using a spectrophotometer. The GST-BCNU activity was expressed as the amount of nitrite moles formed per unit weight of protein per unit of time (nmol/min/mg protein).

DMD #17905

Measurement of plasma BCNU concentration after a single intraperitoneal administration of BCNU

Gstt1-null mice and the wild-type controls were treated via a single intraperitoneal administration with 20 mg/mL BCNU dissolved in 5% ethanol/saline solution at dose levels of 20 mg/kg. Approximately 0.5 mL of blood was collected at 5, 15, 30 and 60 min postdose. The blood samples were centrifuged at 10,000 rpm for 2 min at room temperature to prepare the plasma samples. Then, 10 μ L of plasma sample was placed in disposable glass tubes and 465 μ L of 0.1% acetic acid in water was added and vortexed. After adding 25 μ L of ethanol, the solution was applied to 1 mL of Oasis HLB solid phase extraction cartridge (Waters, Milford, MA). The cartridge was washed previously with 1 mL of acetonitrile followed by 1 mL of water. After the sample was loaded, the cartridge was washed with 1 mL of 0.1% acetic acid in water and then eluted with 0.5 ml of 0.1% acetic acid in acetonitrile. The eluted sample was analyzed on a C18 reverse phase column (Sunfire; 3.5 μ m; 2.1 x 50 mm; Waters) using a step gradient of 95% B until 6 min followed by a step gradient of 5% B until 12 min at a flow rate of 0.2 ml/min. The column effluent was directed into the electrospray ionization (ESI) source of a QTRAP mass spectrometer (MDS Sciex, Toronto, ON, Canada). The ESI conditions were: assist gas flow rate, 85 L/min; evaporation gas, 85 L/min; ionization voltage, -4.5 kV; evaporation temperature, 300°C; field voltage, -0.3 V; and collision energy, -6 V. The data were acquired in negative ion mode using Analyst software (MDS Sciex). BCNU was detected as ion pairs at m/z 271.9/211.9.

Statistical analyse

All data were analyzed by an *F*-test to evaluate the homogeneity of variance. If the variance was homogeneous, a Student's *t*-test was applied. If the variance was heterogeneous, an

DMD #17905

Aspin-Welch's *t*-test was performed. The value of $P < 0.05$ was chosen as an indication of statistical significance except hepatic protein expression analysis. Microsoft Excel (Microsoft Corporation) was used for statistical analysis.

DMD #17905

Results

Generation of *Gstt1*-null Mice

Mice with a disrupted *Gstt1* gene were generated by a homologous recombination method with mouse ES cell. The targeting vector used in this study is shown in Figure 1A. Mouse *Gstt1* gene consists of 5 exons in a region of about 5 kb. This targeting vector was designed to achieve the deletion of exons 1 and 2 of the *Gstt1* gene by replacing them with a Neo^r cassette. W9.5 ES cells were electroporated with the targeting vector and 306 of the colonies with G418 resistance were selected and screened by PCR for homologous recombination. Six independent PCR-positive clones, 1A3, 2A2, 3C6, 9D5, 11D4 and 12B6, were obtained by primary PCR screening with a NeoF3/T1R1 primer pair. However, secondary PCR screening with a GT43/NP3 primer pair revealed that the 12B6 clone was not integrated into the targeted sequence by homologous recombination (data not shown). Chimera mice were generated using the 9D5 ES cell clone with near-diploid karyotype. The F1 offspring were confirmed to succeed to the homologous recombinant allele (Figure 1B). The F1 heterozygous mice were intercrossed to produce F2 mice, which were determined to be wild-type, heterozygote or homozygote (*Gstt1*-null mice) by PCR genotyping (Figure 2). Furthermore, RT-PCR analysis showed *Gstt1* mRNA expression was not detected in the livers of *Gstt1*-null mice (Figure 2). *Gstt1*-null mice appeared to be normal and were as fertile as the wild-type and heterozygote mice. No obvious histological, hematological and blood chemical differences in the basal condition were detected between *Gstt1*-null mice and the wild-type controls (data not shown).

Hepatic protein expression analysis by 2D-DIGE/MS

Hepatic protein expression analysis by 2D-DIGE/MS is summarized in Table 1. The

DMD #17905

expression levels of the 3, 16, and 4 proteins were significantly different between *Gstt1*-null mice and the heterozygotes, the *Gstt1*-null mice and the wild-type control, and the heterozygotes and the wild-type controls, respectively. Among them, the expression levels of the 2 proteins were significantly different between all the genotypes. These proteins were identified as GSTT1 and Albumin 1 by MALDI-TOF MS. In particular, GSTT1 protein was absent in *Gstt1*-null mice (Figure 3). Although we succeeded in the identification of 13 proteins among the 16 proteins which showed significant differences in the expression level between *Gstt1*-null mice and the wild-type controls, the other GSTs were not among them.

GST activities toward CDNB, EPNP, DCM and BCNU in the cytosols of the liver and kidney

We measured the GST-CDNB, GST-EPNP, GST-DCM and GST-BCNU activity in cytosolic samples from the livers and kidneys of *Gstt1*-null mice. The results showed significantly low activity of GST-EPNP, GST-DCM and GST-BCNU in *Gstt1*-null mice, in spite of the same level of GST-CDNB activity in all the genotypes (Figure 4). The GST-EPNP activity of *Gstt1*-null mice was low in the livers of the males (42.1% of the wild-type control), and markedly low in the livers of the females (8.7% of the wild-type control) and in the kidneys of both sexes (male: 27.7%, female: 18.3% of the wild-type control). The GST-DCM activity of *Gstt1*-null mice was nearly absent in the livers and kidneys of both sexes. The GST-BCNU activity of *Gstt1*-null mice was 13.2 – 23.9% of the wild-type control in the livers and kidneys of both sexes. The heterozygotes showed intermediate activity of GST-EPNP, GST-DCM and GST-BCNU between that of the homozygotes and wild-type controls, except for the GST-EPNP and GST-BCNU activity of the female kidney.

DMD #17905

Plasma BCNU concentration after single intraperitoneal administration of BCNU

We measured the plasma concentrations of BCNU after a single intraperitoneal administration of BCNU (20 mg/kg) to *Gstt1*-null mice and the wild-type controls by LC-MS/MS, to evaluate the pharmacokinetics of BCNU in the whole body. This result is shown in Figure 5. The AUC_{5-60 min} was 1102.79 ng·h/mL in the male wild-type controls, 2534.25 ng·h/mL in the male *Gstt1*-null mice, 768.13 ng·h/mL in the female wild-type controls, and 1752.54 ng·h/mL in the female *Gstt1*-null mice. After a single intraperitoneal administration of BCNU to *Gstt1*-null mice, the plasma concentration of BCNU was significantly higher (male, 1.50, 1.93, 4.12, and 3.48 times; female, 1.68, 2.88, 2.57, and 2.44 times at 5, 15, 30, and 60 min, respectively, versus the wild-type controls) and there was a larger AUC_{5-60 min} (male, 2.30 times; female, 2.28 times, versus the wild-type controls) based on the results.

DMD #17905

Discussion

In this study, we generated *Gstt1*-null mice by homologous recombination in order to evaluate the metabolic properties of GSTT1 to the specific substrates. Homologous recombinant ES clones with the predicted mutant allele, confirmed by genomic PCR and direct sequencing analyses, was used to generate mice with a disrupted *Gstt1* gene. Expression analysis by RT-PCR and 2D-DIGE/MS showed that *Gstt1* mRNA expression and GSTT1 protein expression were absent in the *Gstt1*-null mice. These results indicated success in the generation of *Gstt1*-null mice which failed to express *Gstt1* mRNA and GSTT1 protein.

It has been reported that in *Gsta4* knockout mice and *Gstz1* knockout mice the disruption of the *Gst* genes influences the expression level of other GST isoform genes or proteins. This expression change indicates that the disruption of the *Gst* gene may cause a chronic increase in oxidative stress (Engle *et al.*, 2004; Lim *et al.*, 2004). In fact, these knockout mice lines showed an increase in the expression levels of antioxidant enzymes, as well as other GST isoform genes or proteins. In the *Gstt1*-null mice, 2D-DIGE/MS analysis was conducted in order to evaluate the global protein expression in the liver. This result showed that the GSTT1 protein was absent in *Gstt1*-null mice, and that the expression levels of other GSTs were not different between the *Gstt1*-null mice and the wild-type controls. On the other hand, we also found that the expression level of Albumin 1 was different between all the genotypes. The significance of this Albumin expression change is not clear, but we observed that plasma albumin concentration and plasma albumin/globulin ratio were not significantly different between *Gstt1*-null mice and the wild-type control. Furthermore, we succeeded in the identification of 13 proteins among the 16 proteins which showed significant differences in the expression level between *Gstt1*-null mice and the

DMD #17905

wild-type controls. Although 4 proteins among them (Protein disulfide isomerase-related protein, Aflatoxin B1 aldehyde reductase 1, Carbonic anhydrase 3 and Glutathione peroxidase) were reported to cause an increase in the expression levels by oxidative stress (Kyng *et al.*, 2003; Ellis *et al.*, 2003; Engle *et al.*, 2004; Yamamoto *et al.*, 2006), we observed that the expression levels of Aflatoxin B1 aldehyde reductase 1 and Carbonic anhydrase 3 were decreased in *Gstt1*-null mice. Therefore, these results suggest that GSTT1-deficiency does not necessarily cause an increase in oxidative stress under basal conditions.

In the cytosolic study, GST-CDNB activity, a general GST activity, in the liver and kidney was not different between the *Gstt1*-null mice and the wild-type control. This result was consistent with the low GST-CDNB activity of mouse recombinant GSTT1 protein (Whittington *et al.*, 1999). Furthermore, we also observed that P450 activity, assessed by measurement of 7-alkoxycoumarin *O*-dealkylase (ACD) activity using a microsomal fraction, was not different between the *Gstt1*-null mice and the wild-type controls (data not shown). The GST-EPNP activity of the *Gstt1*-null mice was low in the liver and kidney of both sexes. However, the remaining GST-EPNP activity of the *Gstt1*-null mice ranged from 8.7% to 42.1% in the liver, and from 18.3% to 27.7% in the kidney. This result suggests that EPNP is metabolized by not only GSTT1, but also by other xenobiotic metabolizing enzymes. Actually, it has been reported that EPNP is also metabolized by GSTA3, GSTA4, GSTM1, GSTM4, GSTP1 and GSTT3 (Jowsey *et al.*, 2003). The expression level of GSTP1 in the liver was observed to be higher in males than in females, whereas that in the kidney was not different between both sexes (Mitchell *et al.*, 1997). We suppose that GSTP1 may contribute to the higher remaining GST-EPNP activity in the male liver. On the other hand, the GST-DCM activity was nearly absent in the liver and kidney of both

DMD #17905

sexes in the *Gstt1*-null mice. Similar to *Gstt1*-null mice, humans with *GST*-null genotype also showed loss of GST-DCM activity in the cytosol of the liver and kidney (Their *et al.*, 1998).

These results suggest that DCM is a high specific substrate to GSTT1 from mice to humans.

The GST-BCNU activity of *Gstt1*-null mice was markedly low in the liver and kidney of both sexes. In humans, GSTT1, GSTM2 and GSTM3 have GST-BCNU activity, and GSTT1 was demonstrated to have 14-fold higher GST-BCNU activity than GSTM2 and GSTM3 (Lien *et al.*, 2002). In this study, we also observed that GSTT1 was the most efficient catalyst in the liver and kidney cytosols of mice. The remaining GST-BCNU activity of *Gstt1*-null mice ranged from 13.2% to 19.9% in the liver, and from 21.8% to 23.9% in the kidney. We suppose that the other GSTs contribute to the remaining GST-BCNU activity, which may be mouse counterparts of human GSTM2 and GSTM3. Furthermore, we measured the plasma BCNU concentrations after a single intraperitoneal administration of BCNU (20 mg/kg) to *Gstt1*-null mice and the wild-type controls by HPLC-MS/MS, to evaluate the pharmacokinetics of BCNU in the whole body. This result showed that plasma BCNU concentrations after a single intraperitoneal administration of BCNU to *Gstt1*-null mice were significantly higher than those of the wild-type controls, and that there was a larger AUC_{5-60 min} (male, 2.30 times; female, 2.28 times, versus the wild-type controls) based on these results. Considering these results, *Gstt1*-null mice administered a specific substrate for GSTT1, such as BCNU, are highly exposed and toxicologically susceptible to the substrate. In humans, GSTT1 is expressed in the brain, a clinical target for BCNU treatment (Juronen *et al.*, 1996; Sherratt *et al.*, 1997). Therefore, the existence of a *GSTT1*-null genotype may influence both the sensitivity of tumors to BCNU and the severity of the adverse side-effects of BCNU in patients.

DMD #17905

In conclusion, we generated knockout mice for the *Gstt1* gene and found that GST-EPNP, GST-DCM and GST-BCNU activity in the liver and kidney cytosols markedly decreased in *Gstt1*-null mice, and that a single intraperitoneal administration of BCNU to *Gstt1*-null mice resulted in larger AUC_{5-60 min} for the plasma BCNU concentration. Finally, we concluded that *Gstt1*-null mice would be useful as a toxicokinetically modified animal model, i.e. an animal model of a poor metabolizer to the specific substrates for GSTT1, such as an individual with a GSTT1-null genotype. Although the activity, expression level and distribution of GSTT1 are markedly different between humans and mice (Mainwaring *et al.*, 1996; Their *et al.*, 1998), we believe that *Gstt1*-null mice would offer great advantages in determining the roles of GSTT1 in physiological homeostasis, drug metabolism and cancer susceptibility.

DMD #17905

Acknowledgements

We would like to thank S. Yamauchi, H. Kisino, S. Takeshita, Y. Shibaya, Y. Aida and C. Kazama for their excellent technical assistance and Mr. Philip Snider for the proofreading of this manuscript.

DMD #17905

References

- Board PG, Coggan M, Chelvanayagam G, Easteal S, Jermiin LS, Shulte GK, Danley DE, Hoth LR, Griffor MC, Kamath AV, Rosner MH, Chrnyk BA, Perregaux DE, Gabel CA, Geoghegan KF and Pandit J (2000) Identification, characterization, and crystal structure of the omega class glutathione transferases. *J Biol Chem* **275**:24798-24806.
- Board PG, Baker RT, Chelvanayagam G and Jermiin LS (1997) Zeta, a novel class of glutathione transferases in a range of species from plants to humans. *Biochem J* **328**:929-935.
- Bodell WJ, Aida T, Berger MS and Rosenblum ML (1986) Increased repair of O6-alkylguanine DNA adducts in glioma-derived human cells resistant to the cytotoxic and cytogenetic effects of 1,3-bis(2-chloroethyl)-1-nitrosourea. *Carcinogenesis* **7**:879-883.
- Bodell WJ, Rupniak HT, Rasmussen J, Morgan WF and Rosenblum ML (1984) Reduced level of DNA cross-links and sister chromatid exchanges in 1,3-bis(2-chloroethyl)-1-nitrosourea-resistant rat brain tumor cells. *Cancer Res* **44**: 3763-3767.
- Chen CL, Liu Q and Relling MV (1996) Simultaneous characterization of glutathione S-transferase M1 and T1 polymorphisms by polymerase chain reaction in American whites and blacks. *Pharmacogenetics* **6**:187-191.
- Ellis EM, Slattwry CM and Hayes JD (2003) Characterization of the rat aflatoxin B1 aldehyde reductase gene, AKR7A1. Structure and chromosomal localization of AKR7A1 as well as identification of antioxidant response elements in the gene promoter. *Carcinogenesis* **24**: 727-737.
- Engle MR, Singh SP, Czernik PJ, Gaddy D, Montague DC, Ceci JD, Yang Y, Awasthi S, Awasthi

DMD #17905

YC and Zimniak P (2004) Physiological role of mGSTA4-4, a glutathione S-transferase metabolizing 4-hydroxynonenal: generation and analysis of *mGsta4* null mouse. *Toxicol Appl Pharmacol* **194**: 296-308.

Fujimoto K, Arakawa S, Shibaya Y, Miida H, Ando Y, Yasumo H, Hara A, Uchiyama M, Iwabuchi H, Takasaki W, Manabe S and Yamoto T (2006) Characterization of phenotypes in *Gstm1*-null mice by cytosolic and *in vivo* metabolic studies using 1,2-dichloro-4-nitrobenzene. *Drug Metab Dispos* **34**:1495-1501.

Habig WH, Pabst MJ and Jakoby WB (1974) Glutathione S-transferases. The first enzymatic step in mercapuric acid formation. *J Biol Chem* **249**:7130-7139.

Jowsey IR, Thomson AM, Flanagan JU, Murdock PR, Moore GBT, Meyer DJ, Murphy GJ, Smith SA and Hayes JD (2001) Mammalian class Sigma glutathione S-transferases: catalytic properties and tissue-specific expression of human and rat GSH-dependent prostaglandin D₂ synthases. *Biochem J* **359**:507-516.

Jowsey IR, Thomson AM, Orton TC, Elcomve CR, Hayes JD (2003) Biochemical and genetic characterization of a murine class Kappa glutathione S-transferase. *Biochem J* **373**:559-569.

Juronen E, Tasa G, Uuskula M, Pooga M and Mikelsaar AV (1996) Purification, characterization and tissue distribution of huma class theta glutathione S-transferase T1-1. *Biochem Mol Biol Int.* **39**:21-29.

Kyng KJ, May A, Brosh RM Jr, Cheng WH, Chen C, Becker KG and Bohr VA (2003) The transcriptional response after oxidative stress is defective in Cockayne syndrome group B cells. *Oncogene* **22**:1135-1149.

DMD #17905

Landi S (2000) Mammalian class theta GST and differential susceptibility to carcinogens: a review. *Mutat Res* **463**:247-283.

Lim CE, Matthaei K, Blackburn AC, Davis RP, Dahlstrom JE, Koina ME, Anders MW and Board PG (2004) Mice deficient in glutathione transferase zeta/maleylacetoacetate isomerase exhibit a range of pathological changes and elevated expression of alpha, mu and pi class glutathione transferases. *Am J Pathol* **165**: 679-693.

Lowry OH, Rosebrough HJ, Farr AL and Randall RJ (1951) Protein measurement with the folin phenol reagent. *J Biol Chem* **193**:265-275.

Lien S, Larsson AK and Mannervik B (2002) The polymorphic human glutathione transferase T1-1, the most efficient glutathione transferase in the denitrosation and inactivation of the anticancer drug 1,3-bis(2-chloroethyl)-1-nitrosourea. *Biochem Pharmacol* **63**:191-7.

Mainwaring GW, Williams SM, Foster JR, Tugwood J and Green T (1996) The distribution of theta-class glutathione S-transferases in the liver and lung of mouse, rat and human. *Biochem J* **318**:297-303.

Mannervik B, Alin P, Guthenberg C, Jensson H, Tahir MK, Warholm M and Jornvall H (1985) Identification of three classes of cytosolic glutathione transferase common to several mammalian species: Correlation between structural data and enzymatic properties. *Proc Natl Acad Sci USA* **82**:7202-7206.

Meyer DJ, Christodoulides LG, Tan H and Ketterer B (1984) Isolation, properties and tissue distribution of rat glutathione transferase E. *FEBS Lett* **173**:327-330.

Meyer DJ, Coles B, Pemble SE, Gilmore KS, Fraser GM and Ketterer B (1991) Theta, a new class of glutathione transferases purified from rat and man. *Biochem J* **274**:409-414.

DMD #17905

Mitchell AE, Morin D, Lakritz J and Jones AD (1997) Quantitative profiling of tissue- and gender-related expression of glutathione S-transferase isoenzymes in the mouse.

Biochem J **325**: 207-216.

Nash T (1953) The colorimetric estimation of formaldehyde by means of the Hantzsch reaction.

Biochem J **55**:416-421.

Nelson HH, Wiencke JK, Christiani DC, Cheng TJ, Zuo ZF, Schwartz BS, Lee BK, Spitz MR, Wang M and Xu X (1995) Ethnic differences in the prevalence of the homozygous deleted genotype of glutathione S-transferase theta, *Carcinogenesis* **16**:1243-1245.

Sherratt PJ, Pulford DJ, Harrison DJ, Green T and Hayes JD (1997) Evidence that human class Theta glutathione S-transferase T1-1 can catalyse the activation of dichloromethane, a liver and lung carcinogen in the mouse. Comparison of the tissue distribution of GST

T1-1 with that of classes Alpha, Mu and Pi GST in human. *Biochem J* **326**: 837-846.

Smith MT, Evans CG, Doane-Setzer P, Castro VM, Tahir MK and Mannervik B (1989) Denitrosation of 1,3-bis(2-chloroethyl)-1-nitrosourea by class mu glutathione

transferases and its role in cellular resistance in rat brain tumor cells. *Cancer Res* **49**: 2621-2625.

Talcott RE and Levin VA (1983) Glutathione-dependent denitrosation of N,N'-bis(2-chloroethyl)N-nitrosourea (BCNU): nitrite release catalyzed by mouse liver

cytosol in vitro. *Drug Metab Dispos* **11**: 175-176.

Thier R, Wiebel FA, Hinkel A, Burger A, Bruning T, Morgenroth K, Senge T, Wilhelm T and Schulz T (1998) Species differences in the glutathione transferase GSTT1-1 activity

towards the model substrates methyl chloride and dichloromethane in liver and kidney.

DMD #17905

Arch Toxicol **72**:622-629.

Wasserman TH, Slavik M and Carter SK (1975) Clinical comparison of the nitrosoureas. *Cancer* **36**: 1258-1268.

Whittington AT, Vichai V, Webb GC, Baker RT, Pearson WR and Board PG (1999) Gene structure, expression and chromosomal localization of murine Theta class glutathione transferase mGSTT1-1. *Biochem J* **337**:141-151.

Wood SA, Allen ND, Rossant J, Auerbach A and Nagy A (1993) Non-injection methods for the production of embryonic stem cell-embryo chimaeras. *Nature* **365**:87-89.

Yamamoto T, Kikkawa R, Yamada H and Horii I (2006) Investigation of proteomic biomarkers in in vivo hepatotoxicity study of rat liver: Toxicity differentiation in hepatotoxicants. *J Toxicol Sci* **31**:49-60.

DMD #17905

Figure Legends

Figure 1. Targeted disruption of the mouse *Gstt1* gene.

A. The targeting vector construct (top), the wild allele of the *Gstt1* gene (middle), and the predicted mutant allele (bottom) are shown. The targeting vector was constructed by replacing the exon 1 (E1) and exon 2 (E2) of the *Gstt1* gene with a neomycin-resistant (Neo^r) cassette. The *Diphtheria toxin A chain* gene (DT) fragment was ligated at the 5' end of the vector for negative selection. The mutant allele was detectable by PCR using the indicated primer sets, GT43/NP3 and NeoF3/T1R1, which confirmed the homologous recombination on the 5' and 3' arm, respectively. B, PCR analyses of the homologous recombination on the 5' and 3' arm. GT43/NP3 primer set was amplified by a 5.1-kb fragment contained in the 5' arm on the mutant allele (left). NeoF3/T1R1 primer set was amplified by a 2.7-kb fragment contained in the 3' arm on the mutant allele (right). Lambda/HindIII digest was used as a molecular size marker. WT-ES, intact ES cell. 9D5-ES, the homologous recombinant ES cell clone. WT-F1, F1 pup with the wild allele. Hetero-F1, F1 heterozygote with the mutant allele.

Figure 2. PCR genotyping and RT-PCR analysis of *Gstt1*-null mice.

A. The genotype was determined by PCR using two forward primers distinctive between the wild allele and the mutant allele, and one common reverse primer. The wild allele and the mutant allele indicated a 196-bp fragment and a 154-bp fragment, respectively. B. RT-PCR was performed using the primers specific for the mouse *Gstt1* gene and *b-actin* gene. The *Gstt1* and *b-actin* mRNA expression indicated a 270-bp fragment and a 323-bp fragment, respectively. The amplified fragments were confirmed by direct sequence using the ABI PRISM 3700 DNA

DMD #17905

Analyser. M, Phi X174/HincII digest as a molecular size marker; Homo, homozygote (*Gstt1*-null mice); Hetero, heterozygote; Wild, wild-type control.

Figure 3. Comparative analysis of GSTT1 spot using the 2D gel image and DeCyder software.

A. Representative 2D gel image of GSTT1 (Spot No. 1929). B. 3D visualization analyzed using DeCyder software.

Figure 4. GST-CDNB, GST-EPNP, GST-DCM and GST-BCNU activity in a cytosolic sample of the liver and kidney. Enzymatic activity was measured spectrophotometrically. Open, gray and filled bars indicate wild-type, heterozygote and homozygote, respectively. The values are depicted as the mean \pm S.D. of five mice per group. *, $P < 0.05$; **, $P < 0.01$; ***, $P < 0.005$; ****, $P < 0.001$; significant difference from the wild-type controls. N.D., Not detectable.

Figure 5. Plasma BCNU concentrations after a single-dose intraperitoneal administration of BCNU (20 mg/kg) to *Gstt1*-null mice. Open and filled squares indicate wild-type and *Gstt1*-null mice, respectively. The values are depicted as the mean \pm S.D. of five mice per group.

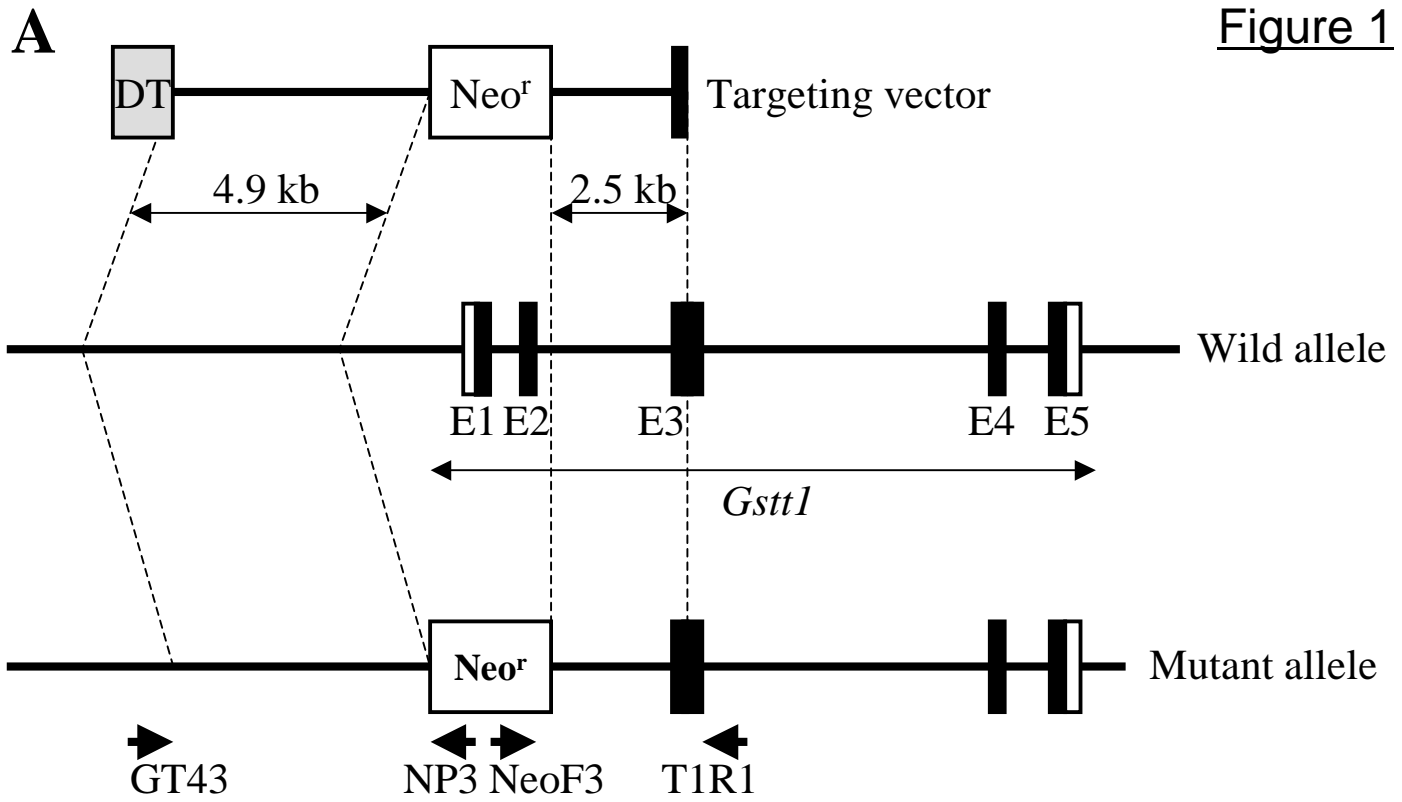
Table 1. List of proteins showing significantly altered expression between *Gstt1*-null mice and the wild-type controls, and identified by MALDI-TOF MS

Spot No.	Identified protein	Homo vs Wild		Hetero vs Wild		Homo vs Hetero	
		Fold change*	P value	Fold change*	P value	Fold change**	P value
320	Methylmalonyl-CoA mutase	0.76	1.3E-03	0.88	0.047	0.86	0.042
382	Histidine ammonia lyase	0.55	2.7E-03	0.86	0.12	0.64	0.031
454	Heat shock protein 8	1.11	1.1E-03	1.06	0.061	1.05	0.100
486	Albumin 1	0.81	2.6E-05	0.92	9.0E-03	0.88	4.3E-03
695	Glucose regulated protein	1.22	1.1E-03	1.10	0.020	1.10	0.036
747	Fibrinogen, beta polypeptide	1.65	5.7E-03	1.29	8.3E-03	1.28	0.094
944	Protein disulfide isomerase-related protein	1.21	2.6E-04	1.08	0.019	1.12	0.011
1328	Aflatoxin B1 aldehyde reductase 1	0.83	2.3E-03	0.91	0.043	0.92	0.088
1443	Glycine N-methyltransferase	1.36	4.7E-04	1.03	0.33	1.31	4.8E-03
1604	Apolipoprotein E	0.83	2.3E-03	0.93	1.3E-03	0.90	0.041
1791	Carbonic anhydrase 3	0.65	4.2E-04	0.88	0.079	0.74	0.019
1929	Glutathione S-transferase, theta 1	0.10	4.2E-05	0.52	2.1E-04	0.18	1.1E-03
2076	Glutathione peroxidase	1.47	3.7E-04	1.09	0.11	1.35	0.011

*: Fold change to the wild-type controls. **: Fold change to the heterozygotes.

The proteins with fold change values shown in bold type were considered to be significantly different ($P < 0.01$) compared to the respective control. Homo, homozygote (*Gstt1*-null mice); Hetero, heterozygote; Wild, wild-type control.

Figure 1



B

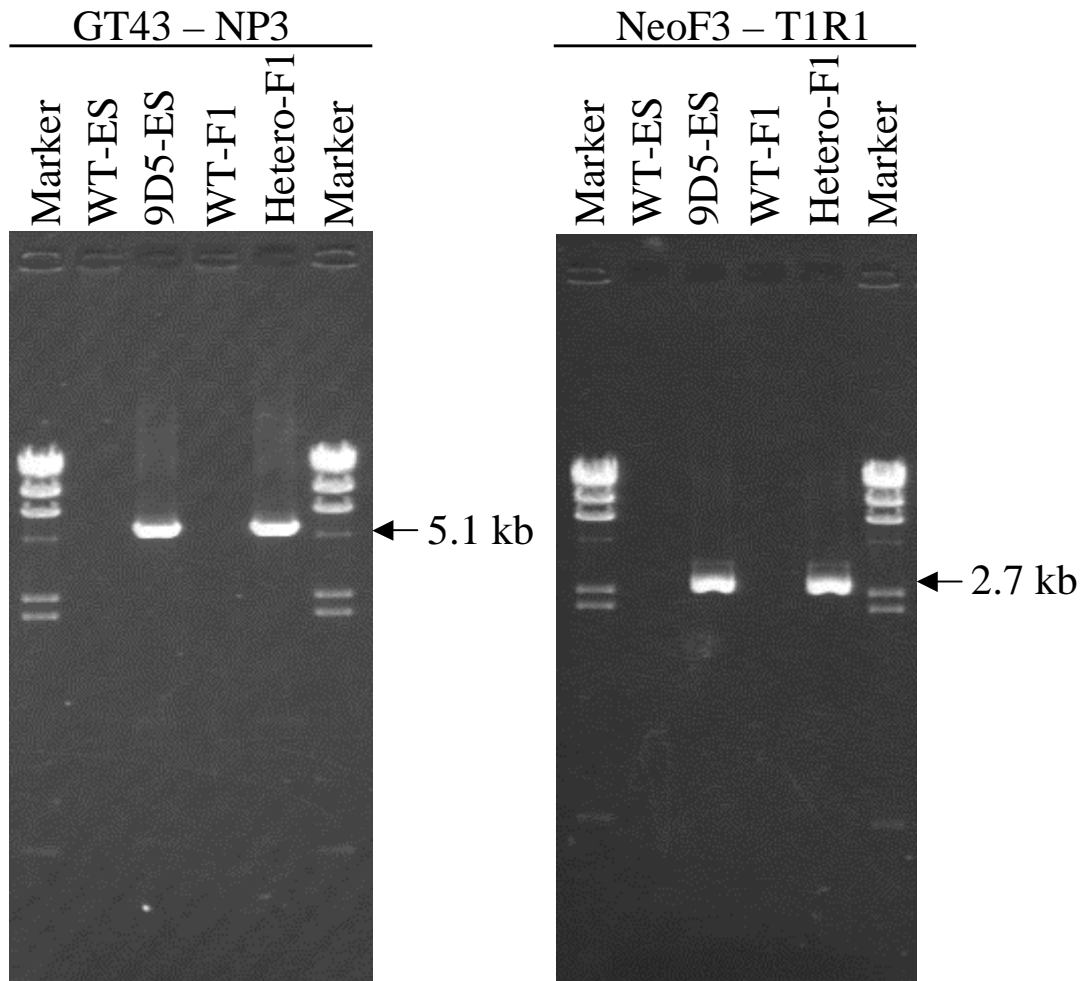


Figure 2

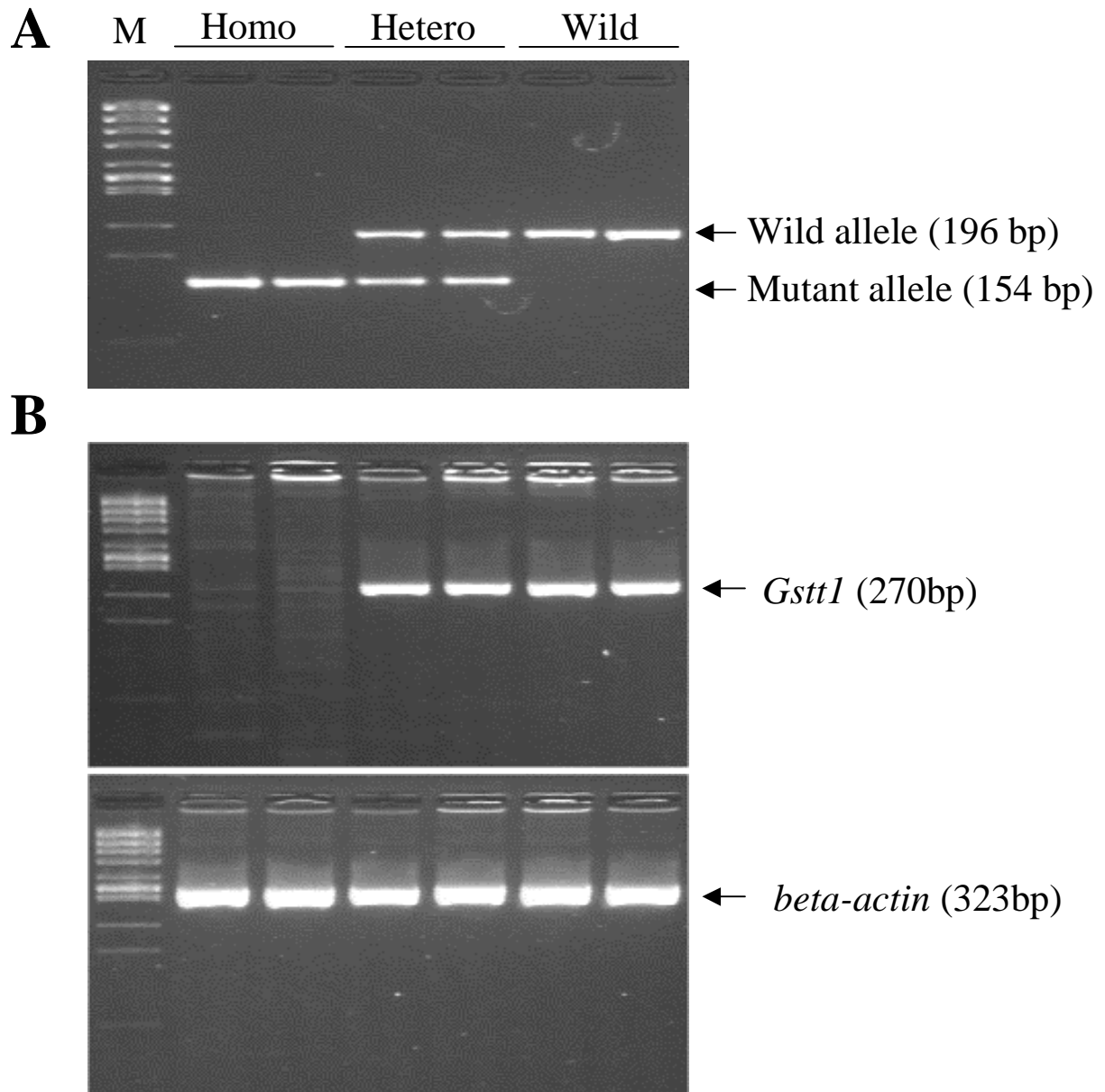


Figure 3

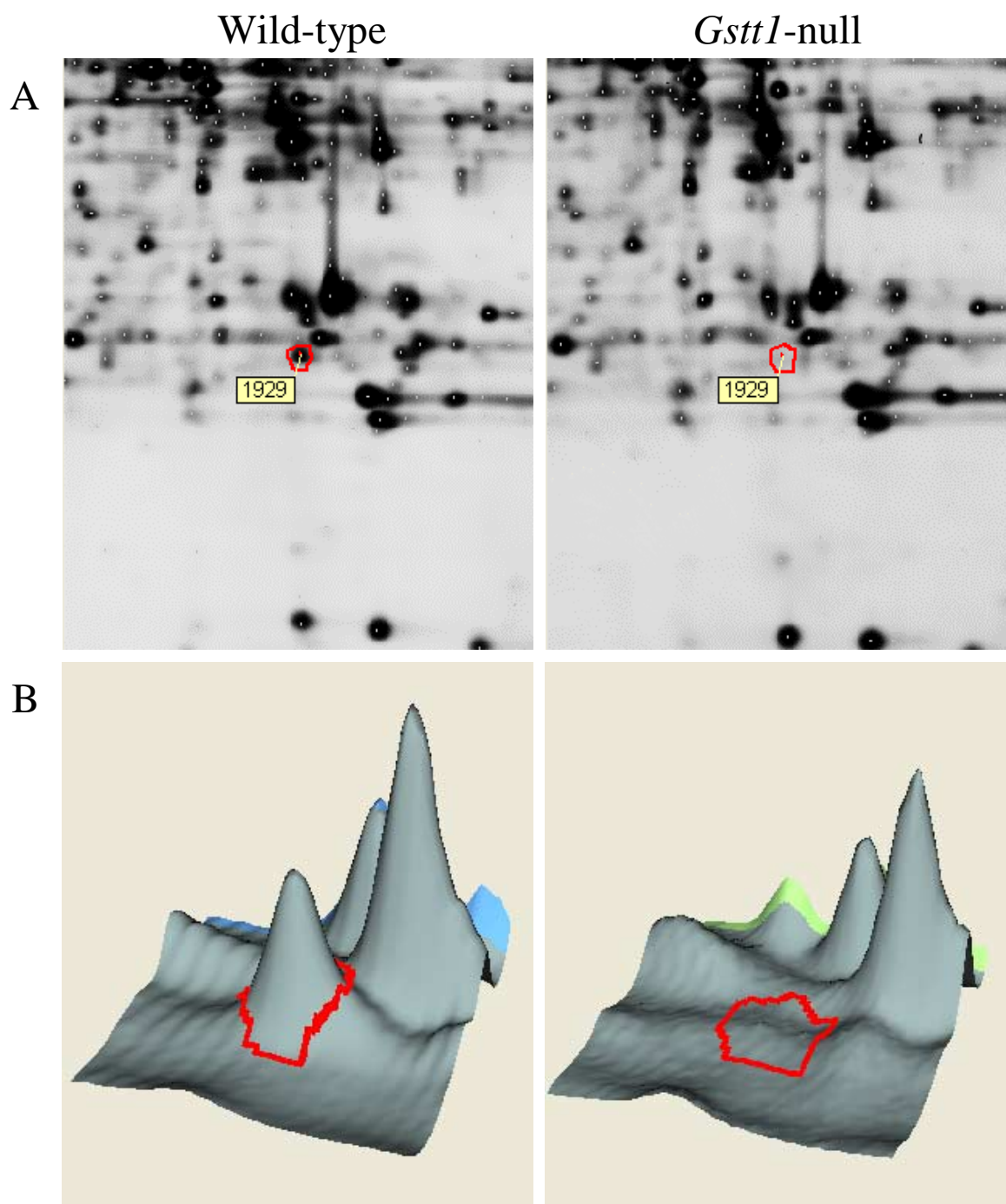


Figure 4

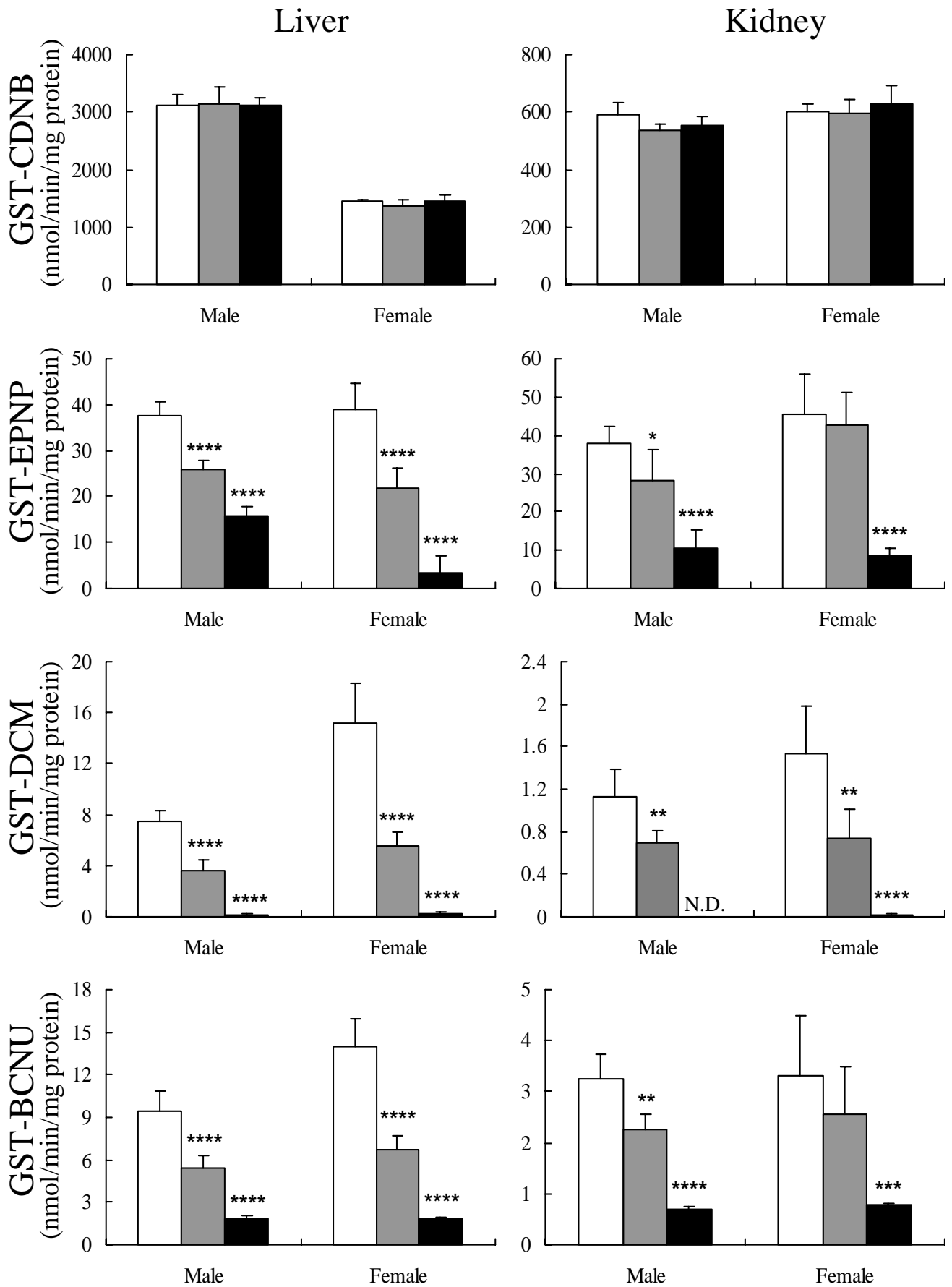


Figure 5

